JOURNAL OF SOLID STATE CHEMISTRY **105**, 392–398 (1993)

The Role of Trivalent Ion in the Metal–Insulator Transition in $(Nd_{0.1}Ca_{0.9})(Mn_{1-x}Al_x)O_3$ and $(Nd_{0.1-y}Ca_{0.9+y})MnO_3$

HIDEKI TAGUCHI* AND MAHIKO NAGAO

Research Laboratory for Surface Science, Faculty of Science, Okayama University, Okayama 700, Japan

Received September 22, 1992; in revised form December 7, 1992; accepted December 9, 1992

The electrical resistivity of the perovskite-types $(Nd_{0.1}Ca_{0.9})(Mn_{1-x}Al_x)O_3$ $(0 \le x \le 0.10)$ and $(Nd_{0.1-y}Ca_{0.9+y})MnO_3$ $(0 \le y \le 0.06)$ was measured in the temperature range 80–800 K. The concentration of the Mn^{3+} ion decreases with increasing x or y. In the range $0 \le x$ or $y \le 0.06$, these systems exhibit the metal–insulator transition. In the metallic region, $d\rho/dT$ increases with decreasing concentration of the Mn^{3+} ion, and is not affected by the Al^{3+} ion. On the other hand, both the metal–insulator transition temperature (T_t) and the energy gap (E_g) calculated from the semiconductive region increase with decreased Mn^{3+} concentration, and are also affected by the Al^{3+} ion.

Introduction

Orthorhombic perovskite-type $CaMnO_3$ exhibits a weak ferromagnetism with $T_N = 123$ K, and an n-type semiconductor (*1*). In recent years, many investigation have been reported on the substitution of the Ca^{2+} ion by the rare earth ion in $CaMnO_3$. According to Jonker and Van Santen (*2*), $(La_{1-x}Ca_x)MnO_3$ was ferromagnetic in the region $0.1 \le x \le 0.5$ (*2*). Taguchi *et al.* measured the electrical properties of $(Ln_{1-x}Ca_x)MnO_3$ (Ln: La, Nd, and Gd) (*3–5*). These manganates exhibit n-type semiconducting behavior below room temperature. At low temperature, the electrical resistivity follows Mott's $T^{-1/4}$ law, indicating the possible occurrence of variable range hopping of electrons due to Anderson localization (*6*). At high temperature, the electrical resistivity of $(Ln_{1-x}Ca_x)MnO_3$ (Ln: La, Nd, and Gd) has a positive temperature coefficient, and the metal–insulator transition of these manganates occurs without any crystallographic change.

The metal–insulator transition temperature (T_t) of $(Ln_{1-x}Ca_x)MnO_3$ (Ln: La, Nd and Gd) decreases with increasing x. At a particular value of x, for which the Mn^{3+}/Mn^{4+} ratio is constant, T_t increases with increasing ionic radius of the rare earth ion. From magnetic measurements of $(Ln_{1-x}Ca_x)MnO_3$ (Ln: La, Nd, and Gd), it is obvious that the spin state of the Mn^{3+} ion changes from low to high at T_t (*3–5*).

In the metallic region of $(Ln_{1-x}Ca_x)MnO_3$ (Ln: La, Nd, and Gd), $d\rho/dT$ monotonically increases with increasing x with little difference between La, Nd, and Gd (*7*). No difference was observed in the $d\rho/dT$–x relation for La, Nd, and Gd, because the number of 3d electrons in the conduction band does not depend on the Ln ion. The number of 3d electrons which exist in the conduction band results from the high-spin state of the Mn^{3+} ion. With increasing x, the number of 3d electrons in the conduction band decreases and $d\rho/dT$ increases.

From these results, it is obvious that the high-spin state of the Mn^{3+} ion plays an important role in controlling the $d\rho/dT$ of $(Ln_{1-x}Ca_x)MnO_3$ (Ln: La, Nd, and Gd).

---

* To whom all correspondence should be addressed.

0022-4596/93 $5.00

In the present study, we tried to synthesize $(Nd_{0.1}Ca_{0.9})(Mn_{1-x}Al_x)O_3$ $(0 \leq x \leq 0.10)$ and $(Nd_{0.1-y}Ca_{0.9+y})MnO_3$ $(0 \leq y \leq 0.06)$ samples. The former is expressed as $(Nd^{3+}_{0.1}Ca^{2+}_{0.9})[Mn^{4+}_{0.9}(Mn^{3+}_{0.1-x}Al^{3+}_x)]O_3$. As the Al^{3+} ion has no $3d$ electron, the number of $3d$ electrons in the conduction band decreases with x. The latter is expressed as $(Nd^{3+}_{0.1-y}Ca^{2+}_{0.9+y})(Mn^{4+}_{0.9+y}Mn^{3+}_{0.1-y})O_3$. The concentration of the Mn^{3+} ion or the number of $3d$ electrons in these systems is the same when $x = y$, and decreases with increasing x or y. The difference between these systems is the presence of the Al^{3+} ion in the former system. Then, we measured the electrical properties of these systems. These results provide some information about the effect of the Mn^{3+} ion for $d\rho/dT$ in the metallic region.

Experimental

All $(Nd_{0.1}Ca_{0.9})(Mn_{1-x}Al_x)O_3$ $(0 \leq x \leq 0.10)$ and $(Nd_{0.1-y}Ca_{0.9+y})MnO_3$ $(0 \leq y \leq 0.06)$ samples were prepared by a standard ceramic technique. Powders of Nd_2O_3, $CaCO_3$, MnO_2, and $Al_2O(CH_3COO)_4 \cdot 4H_2O$ were weighed in the appropriate proportions and milled for a few hours with acetone. After the mixed powders were dried at 373 K, they were calcined in air at 1073 K for 24 hr, then fired at 1623 K for 24 hr under a flow of pure oxygen gas. For measuring the electrical resistivity, the powder was pressed into a pellet form under a pressure of 50 MPa, and the pellet was sintered at 1623 K for 12 hr under a flow of pure oxygen gas. The oxygen-deficient samples obtained in this manner were annealed at 973 K under a flow of pure oxygen gas.

The phases of the samples were identified by X-ray powder diffraction (XRD) with monochromatic Cu$K\alpha$ radiation. The cell constants of the samples were determined from high-angle reflections with Si as a standard.

The oxygen content in each sample was determined by the oxidation–reduction (redox) method. After sodium oxalate solution and perchloric acid were added to dissolve the sample in a flask, the solution was titrated with a standard potassium permanganate solution (*8*).

In the temperature range 300–800 K, differential thermal analysis (DTA) and thermogravimetry (TG) of the samples were performed in air. The electrical resistivity of the samples was measured by a standard four-electrode technique in the temperature range 80–800 K.

Results and Discussion

The oxygen content of $(Nd_{0.1}Ca_{0.9})(Mn_{1-x}Al_x)O_{3-\delta}$ $(0 \leq x \leq 0.10)$ and $(Nd_{0.1-y}Ca_{0.9+y})MnO_{3-\delta}$ $(0 \leq y \leq 0.06)$ samples annealed at 973 K under a flow of pure oxygen was determined to be 2.99–3.00 (δ = 0.00–0.01) by the chemical analysis, and independent of the composition (x or y). This result suggests that all manganates are free of oxygen deficiency. In the temperature range 300–800 K, no exothermic or endothermic peaks were found in DTA measurement. We could not find any loss or gain in TG. These facts indicate that all manganates are stable in air below 800 K. XRD patterns of all manganates were completely indexed as the orthorhombic perovskite-type structure.

The relation between the cell constants and the composition (x or y) for these systems is shown in Fig. 1. The cell constants for $(Nd_{0.1}Ca_{0.9})(Mn_{1-x}Al_x)O_3$ decrease linearly with increasing x. Since the concentrations of the Nd^{3+}, the Ca^{2+}, and the Mn^{4+} ions are independent of x in this system, the cell constants are affected by the concentration of both the Mn^{3+} and the Al^{3+} ions. The ionic radii of the Mn^{3+} (low-spin state), the Mn^{3+} ion (high-spin state), and the Al^{3+} ions with a coordination number (CN) of 12 are 0.58 nm, 0.65 nm, and 0.53 nm, respectively (*9*). With increased amounts of the Al^{3+} ion with a small ionic radius, the cell constants decrease linearly as seen in Fig. 1. The cell constants for $(Nd_{0.1-y}Ca_{0.9+y})MnO_3$ also decrease with increasing y. In this system, the

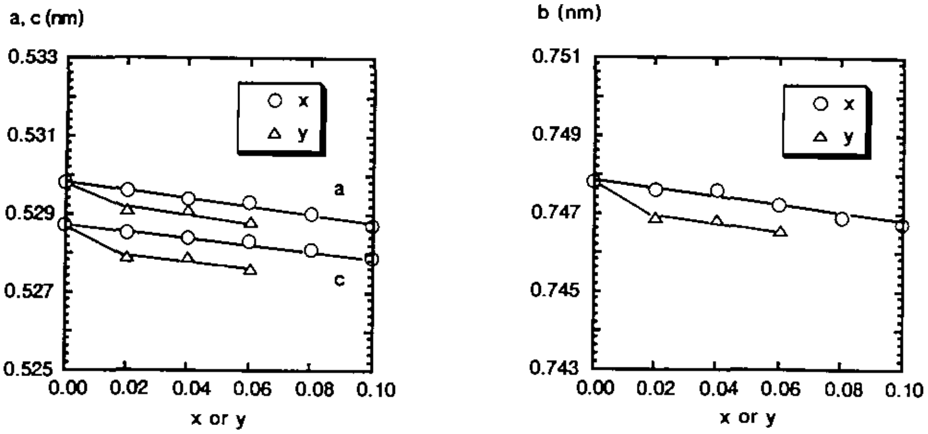

FIG. 1. The relation between the cell constants and the composition (x or y) for $(Nd_{0.1}Ca_{0.9})(Mn_{1-x}Al_x)O_3$ and $(Nd_{0.1-y}Ca_{0.9+y})MnO_3$.

concentration of the Nd^{3+}, Ca^{2+}, Mn^{3+}, and Mn^{4+} ions changes with y. The ionic radius of the Ca^{2+} ion with CN = 12 is 0.135 nm (*9*). Although the ionic radius of the Nd^{3+} ion with CN = 12 is not reported (*9*), it is extrapolated to be ca. 0.10 nm from the results of Shannon and Prewitt (*9*). The cell constants decrease with increasing the Ca^{2+} ion in spite of the fact that the ionic radius of the Ca^{2+} ion is larger than that of the Nd^{3+} ion. The decrease of the cell constants is explained by the increase of the Mn^{4+} ion; that is, the ionic radius of the Mn^{4+} ion with CN = 12 is 0.54 nm and is smaller than that of the Mn^{3+} ion.

Figure 2 shows the reciprocal temperature dependence of the electrical resistivity (ρ) for $(Nd_{0.1}Ca_{0.9})(Mn_{1-x}Al_x)O_3$. $(Nd_{0.1}Ca_{0.9})(Mn_{1-x}Al_x)O_3$ are semiconductors below room temperature. At low temperatures, the slope of log ρ vs $1000/T$ is nonlinear in the region $0 \leq x \leq 0.04$. Figure 3 shows the relation between log ρ and $T^{-1/4}$. In the region $0 \leq x \leq 0.04$, the log ρ vs. $T^{-1/4}$ plot is linear in the temperature range 80 to 110 K, and log ρ strongly depends on x. From these results, it is obvious that the electrical properties of $(Nd_{0.1}Ca_{0.9})(Mn_{1-x}Al_x)O_3$ $(0 \leq x \leq 0.04)$ can be related to variable range hopping of electrons due to Anderson localization in similar to $(Eu_{1-x}Sr_x)$

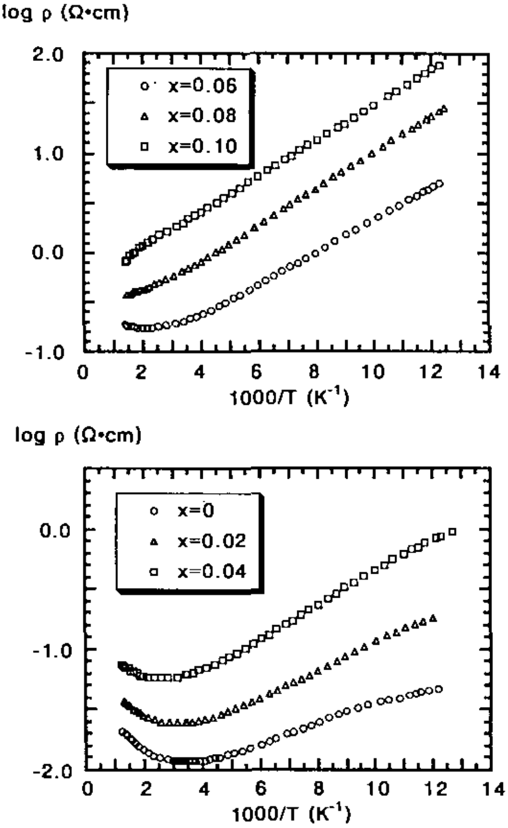

FIG. 2. Electrical resistivity vs $1/T$ for $(Nd_{0.1}Ca_{0.9})(Mn_{1-x}Al_x)O_3$.

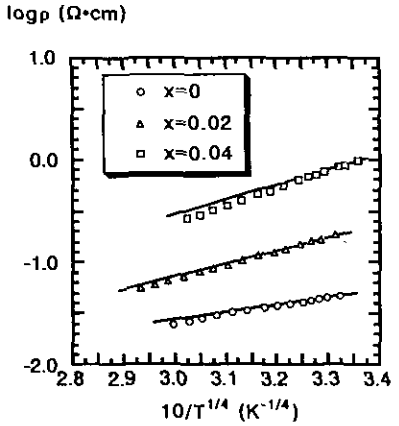

FIG. 3. Electrical resistivity vs $T^{-1/4}$ for $(Nd_{0.1}Ca_{0.9})(Mn_{1-x}Al_x)O_3$.

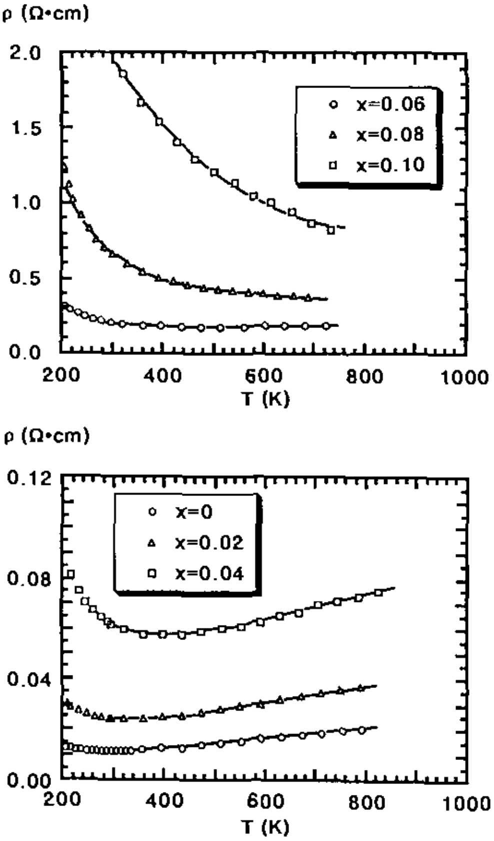

FIG. 5. Electrical resistivity vs T for $(Nd_{0.1}Ca_{0.9})(Mn_{1-x}Al_x)O_3$.

FeO_3 (*6*, *10*). Above 110 K, log ρ vs. $1000/T$ is linear as seen in Fig. 2. We calculated the energy gap (E_g) of $(Nd_{0.1}Ca_{0.9})(Mn_{1-x}Al_x)O_3$ from the linear portion of the log ρ–$1000/T$ curves. Figure 4 shows the relation between E_g and x. E_g monotonically increases with increasing x.

Figure 5 shows the temperature dependence of the electrical resistivity for $(Nd_{0.1}Ca_{0.9})(Mn_{1-x}Al_x)O_3$. In the range $0 \leq x \leq 0.06$, the electrical resistivity has a positive temperature coefficient at high temperature, and increases linearly with increasing temperature. From these results, it is obvious that $(Nd_{0.1}Ca_{0.9})(Mn_{1-x}Al_x)O_3$ exhibits the metal–insulator transition. We define the metal–insulator transition temperature (T_t) as the temperature where the electrical resistivity coefficient changes from negative to positive. The relation between T_t and x is shown in Fig. 6. T_t increases with increasing x. ρ is generally given by

$$\rho = \rho_0 + \rho'\alpha T, \qquad (1)$$

where ρ_0 is a constant which increases with increasing the impurity content, ρ' is a constant and α is a temperature coefficient, and T is temperature (*7*). As we used the sintered manganates to measure the electrical properties, ρ_0 depends on the density of the manganates. In the present study, we used $d\rho/dT$, which is given by

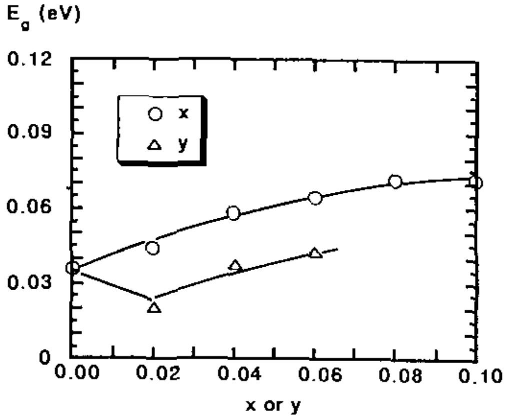

FIG. 4. The relation between the energy gap (E_g) and the composition (x or y) for $(Nd_{0.1}Ca_{0.9})(Mn_{1-x}Al_x)O_3$ and $(Nd_{0.1-y}Ca_{0.9+y})MnO_3$.

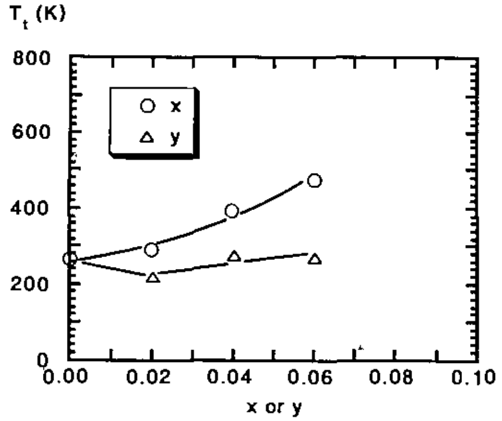

FIG. 6. The relation between the metal–insulator transition temperature (T_t) and the composition (x or y) for $(Nd_{0.1}Ca_{0.9})(Mn_{1-x}Al_x)O_3$ and $(Nd_{0.1-y}Ca_{0.9+y})MnO_3$.

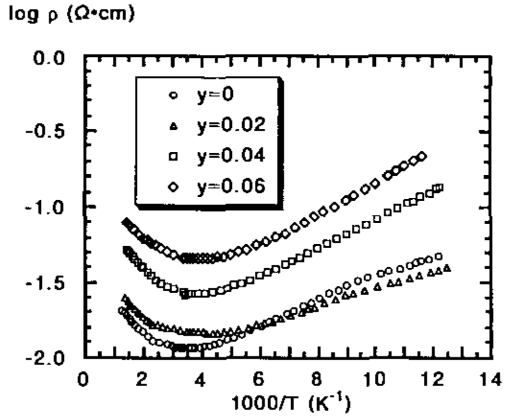

FIG. 8. Electrical resistivity vs $1/T$ for $(Nd_{0.1-y}Ca_{0.9+y})MnO_3$.

$$d\rho/dT = \rho'\alpha, \qquad (2)$$

because it is not easy to get ρ' and α independently. Figure 7 shows the relation between $d\rho/dT$ and x. $d\rho/dT$ linearly increases with x.

Figure 8 shows the reciprocal temperature dependence of the electrical resistivity for $(Nd_{0.1-y}Ca_{0.9+y})MnO_3$. $(Nd_{0.1-y}Ca_{0.9+y})MnO_3$ are semiconductors below room temperature. At low temperature, the slop of log ρ vs. $1000/T$ is nonlinear in the region $0 \leq y \leq 0.02$. Figure 9 shows the relation between log ρ and $T^{-1/4}$. In the region $0 \leq y \leq 0.02$, the relation between log ρ and $T^{-1/4}$ is linear in the temperature range 80 to 110 K, and log ρ strongly depends on y. From these results, it follows that the electrical properties of $(Nd_{0.1-y}Ca_{0.9+y})MnO_3$ are similar to those of $(Nd_{0.1}Ca_{0.9})(Mn_{1-x}Al_x)O_3$.

In both manganate systems, variable range hopping of electrons due to Anderson localization may occur (*6*). The variable range hopping conductivity (σ) for the three-dimensional case is given by

$$\sigma = \sigma_0 \exp[-(T_0/T)^{1/4}], \quad T_0 = \frac{c^4\alpha'^3}{kN(\mu)}, \qquad (3)$$

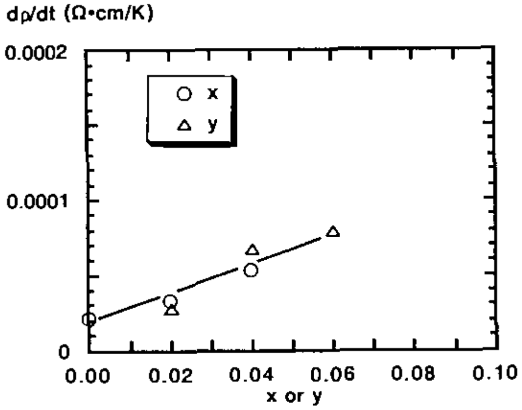

FIG. 7. The relation between $d\rho/dT$ and the composition (x or y) for $(Nd_{0.1}Ca_{0.9})(Mn_{1-x}Al_x)O_3$ and $(Nd_{0.1-y}Ca_{0.9+y})MnO_3$.

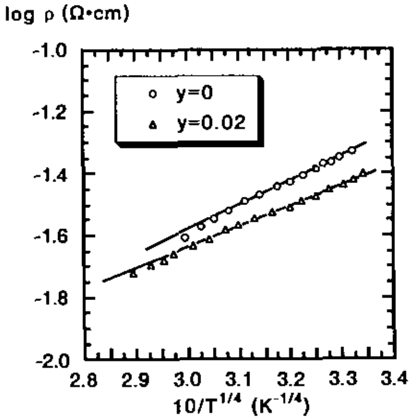

FIG. 9. Electrical resistivity vs $T^{-1/4}$ for $(Nd_{0.1-y}Ca_{0.9+y})MnO_3$.

TABLE I

THE CHARACTERISTIC MOTT TEMPERATURE (T_0) AND THE CRITICAL TEMPERATURE (T_c) FOR NEAREST NEIGHBOR HOPPING OF $(Nd_{0.1}Ca_{0.9})(Mn_{1-x}Al_x)O_3$ AND $(Nd_{0.1-y}Ca_{0.9+y})MnO_3$

Sample	T_0 (K)	T_c (K)
$x = 0.00$	552.8	110.9
$x = 0.02$	926.1	104.2
$x = 0.04$	1035.1	90.9
$y = 0.00$	552.8	110.9
$y = 0.02$	502.5	121.9

where σ_0 is a constant, T_0 is the characteristic Mott temperature, c is the dimensionless constant, α' is the coefficient of exponential decay of the localized state, k is the Boltzmann constant, and $N(\mu)$ is the density of states at the Fermi level (*11*, *12*). The critical temperature (T_c) for nearest neighbor hopping is

$$T_c = \frac{1}{k}\frac{9}{8\pi\alpha' N(\mu)}\left(\frac{4\pi N}{3}\right)^{4/3} \tag{4}$$

where N is the concentration of "the impurity center" participating the hopping motion (*12*). Table I shows the value of T_0 and T_c of both manganate systems. Although T_c of $(Nd_{0.1}Ca_{0.9})(Mn_{1-x}Al_x)O_3$ slightly decreases with increasing x, T_0 largely increases. On the other hand, both T_0 and T_c of $(Nd_{0.1-y}Ca_{0.9+y})MnO_3$ slightly vary with increasing y. These results suggest that the density of states at the Fermi level ($N(\mu)$) decreases by substitution of Mn^{3+} ion by Al^{3+} ion, which has no $3d$ electrons. Above 110 K, the relation between $\log \rho$ and $1000/T$ is linear, as seen in Fig. 8. E_g for $(Nd_{0.1-y}Ca_{0.9+y})MnO_3$, calculated from the linear portion of $\log \rho$–$1000/T$, curves, is also shown in Fig. 4. E_g for $(Nd_{0.1-y}Ca_{0.9+y})MnO_3$ has a minimum value at $y = 0.02$. Then, E_g increases with increasing y in the range $0.02 \leq y \leq 0.06$, although E_g for $(Nd_{0.1-y}Ca_{0.9+y})MnO_3$ is smaller by ca. 0.02 eV than E_g for $(Nd_{0.1}Ca_{0.9})(Mn_{1-x}Al_x)O_3$.

Figure 10 shows the temperature dependence of the electrical resistivity for $(Nd_{0.1-y}Ca_{0.9+y})MnO_3$. At high temperature, the electrical resistivity has a positive temperature coefficient, and increases linearly with increasing temperature. From these results, it is concluded that $(Nd_{0.1-y}Ca_{0.9+y})MnO_3$ exhibits a metal–insulator transition. The relation between T_t and y is shown in Fig. 6. T_t for $(Nd_{0.1-y}Ca_{0.9+y})MnO_3$ has a minimum value at $y = 0.02$. Then, T_t slightly increases with increasing y. The relation between $d\rho/dT$ and y is presented in Fig. 7. Both $(Nd_{0.1}Ca_{0.9})(Mn_{1-x}Al_x)O_3$ and $(Nd_{0.1-y}Ca_{0.9+y})MnO_3$ have the same values of $d\rho/dT$, and $d\rho/dT$ increases with decreasing concentration of Mn^{3+} ion.

When $x = y$, the Mn^{3+} concentration in $(Nd_{0.1}Ca_{0.9})(Mn_{1-x}Al_x)O_3$ and $(Nd_{0.1-y}Ca_{0.9+y})MnO_3$ is identical. With increasing x or y, the concentration of the Mn^{3+} ion decreases. These systems exhibit the metal–insulator transition in the range $0 \leq x, y \leq 0.06$. In the semiconductive region, E_g of $(Nd_{0.1}Ca_{0.9})(Mn_{1-x}Al_x)O_3$ is larger by ca. 0.02 eV than E_g of $(Nd_{0.1-y}Ca_{0.9+y})MnO_3$ as seen in Fig. 4. In Ref. (*7*), we have proposed a simple energy band scheme in which the valence band (π^* orbital) and the conduction band (σ^* orbital) are separated by E_g (or Δ). E_g is strongly affected by temperature, the number of $3d$ electrons, the Mn–O

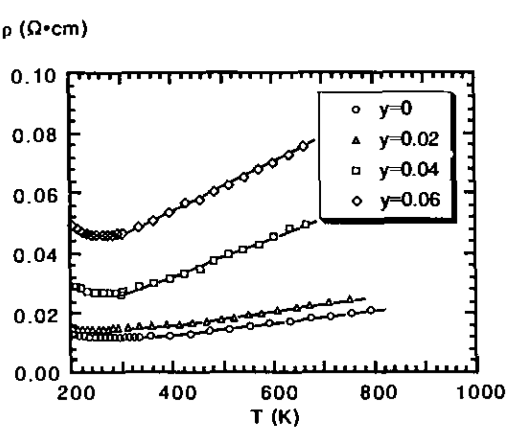

FIG. 10. Electrical resistivity vs T for $(Nd_{0.1-y}Ca_{0.9+y})MnO_3$.

distance, and the impurity concentration. From magnetic measurements on $(Ln_{1-x}Ca_x)MnO_3$ (*Ln*: La, Nd and Gd), it was shown that the Mn^{3+} ions are in the low spin state below T_t (*3–5*), and that there are no 3*d* electrons in the conduction band at low temperature. Since the Mn–O distance of these systems decreases with increasing x or y as seen in Fig. 1, E_g is not strongly affected by the Mn–O distance. Therefore, we consider that the presence of the Al^{3+} ion makes E_g of $(Nd_{0.1}Ca_{0.9})(Mn_{1-x}Al_x)O_3$ large, and the low-spin state of the Mn^{3+} ion becomes stable at high temperature. Consequently, the metal–insulator transition of $(Nd_{0.1}Ca_{0.9})(Mn_{1-x}Al_x)O_3$ occurs at high temperature in comparison with $(Nd_{0.1-y}Ca_{0.9+y})MnO_3$, and T_t for $(Nd_{0.1}Ca_{0.9})(Mn_{1-x}Al_x)O_3$ will be higher than for $(Nd_{0.1-y}Ca_{0.9+y})MnO_3$, as seen in Fig. 6. In the metallic region of these systems, the Mn^{3+} ions are in the high-spin state, and we could not find a difference in $d\rho/dT$ for these systems (Fig. 7). This result supports our assumption that $d\rho/dT$ depends on the number of 3*d* electrons in the conduction band (*7*).

The trivalent ions, both the Mn^{3+} and the Al^{3+} ions, play an important role in controlling the electrical properties of $(Ln_{1-x}Ca_x)MnO_3$. We have to decrease the concentration of the Mn^{3+} ion in order to get higher values of $d\rho/dT$. There are two ways to do so. One is to increase x in $(Ln_{1-x}Ca_x)MnO_3$, and the other is to substitute the Mn^{3+} ion by the Al^{3+} ion in $(Ln_{1-x}Ca_x)MnO_3$. It is shown that $d\rho/dT$ increases with decreasing concentration of the Mn^{3+} ion in both systems, but that the Al^{3+} ions themselves do not influence $d\rho/dT$, although both E_g and T_t are strongly affected by the Al^{3+} ion.

Conclusion

$(Nd_{0.1}Ca_{0.9})(Mn_{1-x}Al_x)O_3$ $(0 \leq x \leq 0.10)$ and $(Nd_{0.1-y}Ca_{0.9+y})MnO_3$ $(0 \leq y \leq 0.06)$ exhibit a metal–insulator transition. The concentration of the Mn^{3+} ion decreases with increasing x or y. Although the concentration of the Mn^{3+} ion in these systems is the same when $x = y$, both E_g and T_t for $(Nd_{0.1}Ca_{0.9})(Mn_{1-x}Al_x)O_3$ are larger than for $(Nd_{0.1-y}Ca_{0.9+y})MnO_3$. Since the Al^{3+} ion in $(Nd_{0.1}Ca_{0.9})(Mn_{1-x}Al_x)O_3$ makes E_g large, the low-spin state of the Mn^{3+} ion is stable at higher temperatures in comparison with $(Nd_{0.1-y}Ca_{0.9+y})MnO_3$. Consequently, the metal–insulator transition occurs at higher temperatures, and T_t for $(Nd_{0.1}Ca_{0.9})(Mn_{1-x}Al_x)O_3$ is higher than that for $(Nd_{0.1-y}Ca_{0.9+y})MnO_3$. In the metallic region, however, there is no difference in $d\rho/dT$ for these systems. $d\rho/dT$ depends on the concentration of the Mn^{3+} ion, that is, the number of 3*d* electrons in the conduction band.

References

1. J. B. MacChesney, H. William, J. F. Potter, and R. C. Sherwood, *Phys. Rev.* **164,** 779 (1967).
2. G. H. Jonker and J. H. van Santen, *Physica* **16,** 337 (1950).
3. H. Taguchi and M. Shimada, *J. Solid State Chem.* **62,** 290 (1986).
4. H. Taguchi, M. Nagao, and M. Shimada, *J. Solid State Chem.* **76,** 284 (1988).
5. H. Taguchi, M. Nagao, and M. Shimada, *J. Solid State Chem.* **82,** 8 (1989).
6. N. F. Mott, *Adv. Phys.* **21,** 785 (1972).
7. H. Taguchi, M. Nagao, and M. Shimada, *J. Solid State Chem.* **97,** 476 (1992).
8. N. Mizutani, N. Okuma, A. Kitazawa, and M. Kato, *Kogyo Kagaku Zasshi* **73,** 1103 (1970). [In Japanese]
9. R. D. Shannon and C. T. Prewitt, *Acta Crystallogr. Sect. B* **25,** 925 (1969).
10. V. Joshi, O. Parakash, G. N. Rao, and C. N. R. Rao, *J. Chem. Soc. Faraday Trans.* **2,** 75 (1979).
11. V. Ambegaokar, B. I. Halperin, and J. S. Langer, *Phys. Rev. B* **4,** 2612 (1971).
12. H. Bottger, and V. V. Bryksin, *Phys. Status Solidi B* **78,** 9 (1976).